

Available online at [www.sciencedirect.com](http://www.sciencedirect.com)

Physics Procedia 3 (2010) 1201–1205

**Physics  
Procedia**[www.elsevier.com/locate/procedia](http://www.elsevier.com/locate/procedia)14<sup>th</sup> International Conference on Narrow Gap Semiconductors and Systems

## Cyclotron Resonance in P-doped InSb Quantum Wells

M.B. Santos<sup>a\*</sup>, M. Edirisooriya<sup>a</sup>, T.D. Mishima<sup>a</sup>, C.K. Gaspe<sup>a</sup>, J. Coker<sup>a</sup>, R.E. Doezeema<sup>a</sup>,  
X. Pan<sup>b</sup>, G.D. Sanders<sup>b</sup>, C.J. Stanton<sup>b</sup>, L.C. Tung<sup>c</sup>, and Y.-J. Wang<sup>c</sup>

<sup>a</sup> Homer L. Dodge Department of Physics & Astronomy, University of Oklahoma, Norman, Oklahoma, USA

<sup>b</sup> Department of Physics, University of Florida, Gainesville, Florida, USA

<sup>c</sup> National High Magnetic Field Laboratory, Florida State University, Tallahassee, Florida, USA

### Abstract

A combined experimental and theoretical study of cyclotron resonance was conducted on a two-dimensional hole system in an InSb quantum well, which was 9 nm thick and compressively strained by ~0.65%. An effective mass of  $0.065m_0$  and a  $g$ -factor of  $|g| \approx 23$  were deduced from cyclotron resonance features at magnetic fields of 2.5T and 6T, respectively, when the InSb quantum well had a hole density of  $3.5 \times 10^{11} \text{ cm}^{-2}$ . At higher magnetic fields, separate cyclotron resonances are observed for different spin-conserving transitions. The magnetic field dependences of the effective mass and  $g$ -factor for holes are well explained by an 8-band Pidgeon-Brown model generalized to include the effects of the confinement potential and pseudomorphic strain.

Keywords: Molecular Beam Epitaxy; Cyclotron Resonance; Narrow Gap Semiconductors

### 1. Introduction

In order to realize high-performance CMOS circuits, both  $n$ -type and  $p$ -type quantum-well (QW) transistors with high room-temperature mobility are necessary. Some III-V QW materials, including GaAs and  $\text{In}_x\text{Ga}_{1-x}\text{As}$  QWs, exhibit high electron mobilities, but have low hole mobilities. In principle, the hole mobility can be increased through compressive strain and by using a material, such as InSb, that has a smaller band gap. InSb  $n$ -type field-effect transistors (FETs) have already exhibited higher switching speeds and lower power consumption than other III-V FETs [1].

\* Corresponding author. Tel. : 405-325-3961. E-mail Address: [msantos@ou.edu](mailto:msantos@ou.edu)

We report on a combined experimental and theoretical study of a two-dimensional (2D) hole system in an InSb QW. The highest room-temperature hole mobility that we have observed in such structures, 700 cm<sup>2</sup>/Vs, and that others have observed in similar structures [2] is higher than observed in *p*-type In<sub>x</sub>Ga<sub>1-x</sub>As QWs [3-5]. It is still, however, lower than the highest values observed for 2D hole systems in QWs made from In<sub>x</sub>Ga<sub>1-x</sub>Sb (1,500 cm<sup>2</sup>/Vs [6]) and Ge (3,100 cm<sup>2</sup>/Vs [7]). The low-temperature hole mobility in the InSb QW used in this study, 22,000 cm<sup>2</sup>/Vs, is sufficient for the observation of cyclotron resonance at magnetic fields as low as 2T. Further manipulation of the structural parameters to increase the strain in the QW is expected to substantially lower the effective mass of holes and, consequently, increase the hole mobility.

## 2. Experiment

The layer structure for our *p*-type InSb QW has been previously reported [8]. In this study, a 2D hole system is confined within a 9 nm-thick InSb QW by Al<sub>0.20</sub>In<sub>0.80</sub>Sb barrier layers. The holes are created by a Be  $\delta$ -doped layer that is 20 nm above the QW layer. The InSb QW is compressively strained by  $\sim 0.65\%$  to the lattice constant of the thick Al<sub>x</sub>In<sub>1-x</sub>Sb buffer layer, which is grown by molecular beam epitaxy on a GaAs (001) substrate. Both confinement and strain are expected to lift the degeneracy of the heavy-hole and light-hole bands at an in-plane wave-number of zero. From Hall-effect and resistivity measurements at 20K, we deduced a hole mobility of 22,000 cm<sup>2</sup>/Vs and a hole density of  $3.5 \times 10^{11} \text{ cm}^{-2}$ .

The effective mass of the holes was characterized through magneto-optical measurements in the Faraday geometry using a Fourier transform infrared spectrometer, with an applied magnetic field up to  $B=17.5$  T, and at a temperature of 4.2K. The experimental data is presented in Figure 1, where the negative of the intensity of transmitted light  $T(B)$  is normalized by dividing by  $T(0)$  and plotted as a function of  $B$  and the photon wavenumber  $q$ . The photon source for the data in Figures 1a and 1b was a mercury lamp and a globar, respectively. A different beam splitter was used for each photon source, while a bolometer was used in both configurations to measure  $T(B)$ . The arrows in Figure 1 indicate transmission features that we ascribe to cyclotron resonance (CR) transitions. In a CR transition, a hole absorbs the energy of a photon to move to a neighbouring Landau level (increase Landau level index by one) with the same spin (no change in spin quantum number). At  $q$  values near the LO phonon frequency for InSb (190 cm<sup>-1</sup>), the CR positions are affected by resonant magneto-polaron coupling. At  $q$  values between about 240 and 310 cm<sup>-1</sup>, the CR features are completely obscured by strong absorption in the *reststrahlung* band of the GaAs substrate.

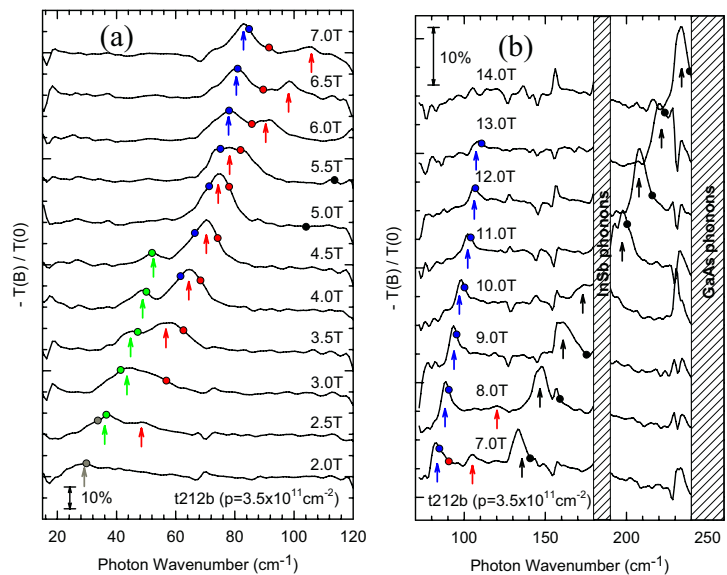


**Fig.1** Normalized negative transmission through a *p*-type InSb QW at 4.2K, as a function of photon wavenumber and applied magnetic field. The arrows and circles mark the CR positions that were experimentally observed and theoretically predicted, respectively.

At  $B \leq 3$  T, where spin splitting cannot be resolved, we observe a single CR feature. From this feature, we deduce a hole effective mass of  $m^* = 0.065m_0$ . This mass is lighter than the  $m^*$  measured for other III-V QWs at comparable hole density, including GaAs ( $0.3m_0$  for  $p = 1.6 \times 10^{11} \text{ cm}^{-2}$  [9]) and  $\text{In}_{0.20}\text{Ga}_{0.80}\text{As}$  ( $0.15m_0$  for  $p = 3 \times 10^{11} \text{ cm}^{-2}$  [10]) and  $\text{In}_{0.23}\text{Ga}_{0.77}\text{Sb}$  ( $0.1m_0$  for  $p = 7.8 \times 10^{11} \text{ cm}^{-2}$  [6]). At higher fields, we observe separate features for different spin-conserving transitions between neighbouring Landau levels.

### 3. Calculation

To explain the CR features at higher  $B$ , calculations of the spin-dependent CR magneto-absorption spectra in a pseudomorphically strained, narrow gap  $\text{Al}_x\text{In}_{1-x}\text{Sb}/\text{InSb}$  QW were performed. Our model for CR magneto-absorption in a QW is based on a modified 8-band Pidgeon-Brown model that incorporates the confinement potential as well as the pseudomorphic strain. In the pseudomorphic strain approximation, the in-plane lattice constant of the QW is taken to be pinned to the lattice constant of the relaxed  $\text{Al}_x\text{In}_{1-x}\text{Sb}$  buffer layer. Details of the theory can be found in References 11, 12 and 13. The magnetic field is taken to be oriented along the QW (001) growth direction  $z$ . In solving the problem, we make use of the axial approximation where we neglect terms that depend on the difference of the Luttinger parameters  $\gamma_2 - \gamma_3$ . Using this approximation, the problem separates into a series of matrices which can be diagonalized independently. Using the Landau gauge, the effective mass Hamiltonian in the QW is a position dependent operator that is separated into Landau and strain contributions and depends explicitly on the Pidgeon-Brown manifold number  $n = -1, 0, 1, \dots$ . For each manifold number  $n$ , a finite difference scheme is used to obtain the subband energies and position dependent effective mass envelope functions in the QW [14].

Figure 2 shows the calculated fan diagram for the spin-split Landau levels (LLs) from the lowest heavy hole subband, with LL indices of  $N = 0, 1, 2, 3$ . The dotted lines correspond to spin down ( $m_j = -3/2$ ) states while the solid lines correspond to spin up ( $m_j = +3/2$ ) states. The effects of mixing between states from different subbands can be seen for the  $\text{H}3\downarrow$  state for fields greater than 8 T. The Fermi energy for  $p = 3.5 \times 10^{11} \text{ cm}^{-2}$  is also plotted. The non-linear  $B$  dependences of the LL energies reflect strong dependences of  $m^*$  and the effective Landé  $g$ -factor,  $g^*$ , on  $B$ . The crossing of dashed and solid lines with the same LL index indicates that even the sign of  $g^*$  can depend on  $B$ . The largest value predicted for  $|g^*|$  is  $\sim 30$ , when  $N = 0$  and  $B = 2$  T. Examples of spin-conserving CR transitions are indicated by arrows in Figure 2. It is apparent that the CR energies will be different for the transitions indicated by black ( $\text{H}0\downarrow$  to  $\text{H}1\downarrow$ ), blue ( $\text{H}0\uparrow$  to  $\text{H}1\uparrow$ ), red ( $\text{H}1\downarrow$  to  $\text{H}2\downarrow$ ), and green ( $\text{H}1\uparrow$  to  $\text{H}2\uparrow$ ) arrows.

Optical properties are calculated within the Fermi golden rule approximation as described in Reference 12. Figure 3 shows the result of

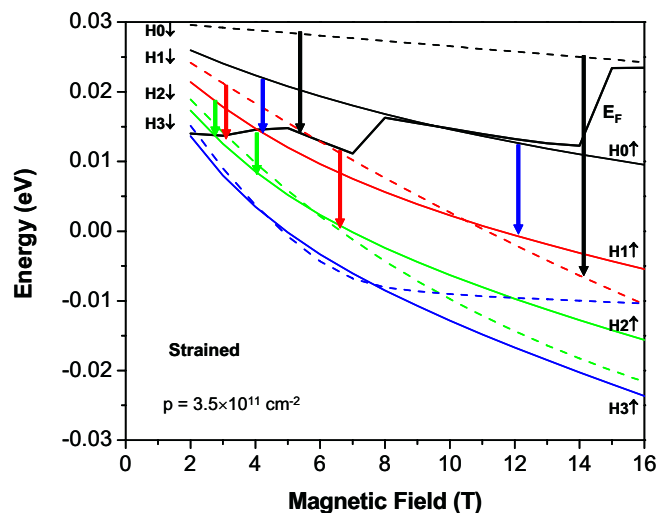


**Fig.2** Calculated Landau-level fan diagram for holes in an InSb QW. Spin-conserving cyclotron transitions are indicated by arrows. The Landau levels are labelled by their  $N$  value (1, 2, or 3) and spin orientation ( $\uparrow$  or  $\downarrow$ ).

our cyclotron absorption calculations when strain is included, Figures 3a and 3b, and when strain is not included, Figures 3c and 3d. The strong dependence on strain can be seen by comparing Figure 3a with 3c and Figure 3b with 3d. The colors of the solid symbols in Figures 3a and 3b indicate which CR transitions from Figure 2 are associated with which calculated absorption features. As can be seen, without the proper inclusion of strain, the calculated CR transitions are substantially different from the experimental results shown in Figure 1. This result is similar to our previous results on valence band to conduction band magneto-absorption where we showed that the inclusion of strain was crucial for obtaining agreement between the experiment and the theoretical modeling [14].

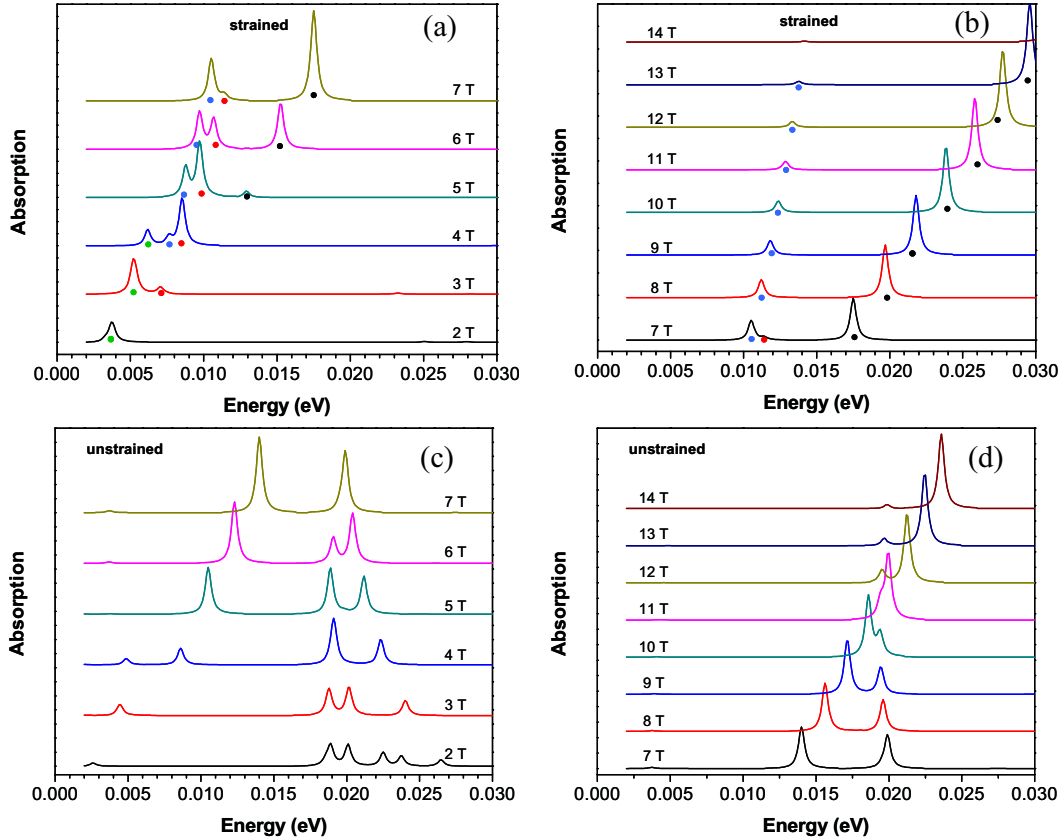


**Fig.3** Calculated CR absorption spectra for a *p*-type InSb quantum well. The calculations are performed (a), (b) with mechanical strain included and (c), (d) with mechanical strain ignored. The solid points in (a) and (b) associate the features with particular transitions shown in Figure 2.

#### 4. Comparison between experiment and calculation

By comparing Figure 1a with Figure 3a and Figure 1b with Figure 3b, one can see that the predicted intensities of the CR absorption features compare reasonably well with the experimentally determined intensities. Figure 4 shows generally good agreement between the predicted (lines) and observed (solid symbols) energies of the CR transitions as functions of  $B$ . We see that the energy of the  $H0\downarrow$  to  $H1\downarrow$  transition is slightly overestimated by the model compared to the experiment. This could result from several effects such as slight errors in the Luttinger parameters used in the calculations or from the fact that the confining potential was not calculated using the self-consistent carrier densities in the well. The only significant disagreement between theory and experiment is in the

energy of the  $H1\downarrow$  to  $H2\downarrow$  transition in the region between  $6\text{ T} < B < 8\text{ T}$ , which is underestimated by the theoretical model. A possible explanation for this discrepancy is a strong anticrossing between the  $H2\uparrow$  and  $H2\downarrow$  states. While our model shows a crossing between these states at  $\sim 5.5\text{ T}$  within the axial approximation, we anticipate that inclusion of cubic as well as Coulombic terms in the Hamiltonian will lead to an anticrossing between these levels. The net effect of this anticrossing is to repel the  $H2\downarrow$  level to more negative energies after the crossing (about  $5.5\text{ T}$ ). This will result in a shift of the cyclotron resonance for the  $H1\downarrow$  to  $H2\downarrow$  transition to higher energies above  $5.5\text{ T}$ . Indeed, this is seen to be the case as shown in Figure 1a.

## 5. Conclusions

Cyclotron resonance experiments indicate an effective mass of  $0.065m_0$  for a hole density of  $3.5 \times 10^{11}\text{ cm}^{-2}$  in a strained InSb quantum well. Spin-resolved CR features at high magnetic fields are well modeled by an 8-band Pidgeon-Brown model that accounts for the confinement potential and pseudomorphic strain. We find that strain has a dramatic effect on the CR magneto-absorption spectra. The model is useful for determining the optimal parameters for achieving a given hole density while minimizing the effective mass.

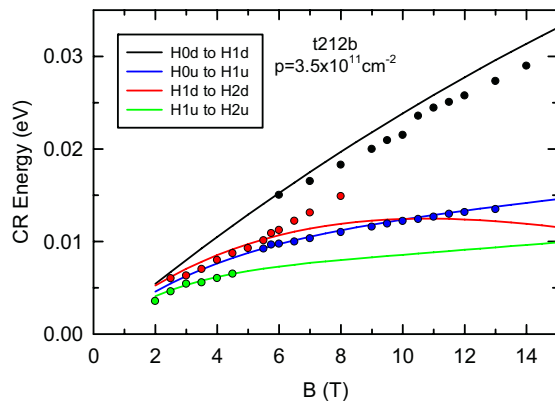


**Fig.4** Observed (solid symbols) and predicted (lines) CR energies as functions of applied magnetic field.

## 6. Acknowledgements

This work was supported by the National Science Foundation through the grants: DMR-0808086, DMR-0520550, DMR-0706313, and OISE-0530220 and the Department of Energy through DE-FG02-02ER45984.

## References

- [1] S. Datta, T. Ashley, J. Brask, L. Buckle, M. Doczy, M. Emeny, D. Hayes, K. Hilton, R. Jefferies, T. Martin, and T.J. Phillips, D. Wallis, P. Wilding, and R. Chau, Proceedings of the 2005 IEEE International Electron Devices Meeting.
- [2] M. Radosavljevic, T. Ashley, A. Andreev, S.D. Coomber, G. Dewey, M.T. Emeny, M. Fearn, D.G. Hayes, K.P. Hilton, M.K. Hudait, R. Jefferies, T. Martin, R. Pillarisetty, W. Rachmady, T. Rakshit, S.J. Smith, M.J. Uren, D.J. Wallis, P.J. Wilding, and R. Chau, Proceedings of the 2008 IEEE International Electron Devices Meeting.
- [3] R.T. Hsu, W.C. Hsu, M.J. Kao, and J.S. Wang, Appl. Phys. Lett. 66, 2864 (1995).
- [4] Y.-J. Chen and D. Pavlidis, IEEE Trans. Elec. Dev. 39, 466 (1992).
- [5] A.M. Kusters, A. Kohl, V. Sommer, R. Muller, and K. Heime, IEEE Transactions on Electron Devices 40, 2164 (1993).
- [6] B.R. Bennett, M.G. Ancona, J.B. Boos, and B.V. Shanabrook, Appl. Phys. Lett. 91, 042104 (2007).
- [7] M. Myronov, K. Sawano, Y. Shiraki, T. Mouri, and K.M. Itoh, Appl. Phys. Lett. 91, 082108 (2007).
- [8] M. Edirisooriya, T.D. Mishima, C.K. Gaspe, K. Bottoms, R.J. Hauenstein, and M.B. Santos, J. Cryst. Growth 311, 1972 (2009).
- [9] K. Rachor, T.E. Raab, D. Heitmann, C. Gerl, and W. Wegscheider, Phys. Rev. B 79, 125417 (2009).
- [10] S.-Y. Lin, H.P. Wei, D.C. Tsui, and J.F. Klem, Appl. Phys. Lett. 67, 2170 (1995).
- [11] Y.D. Jho, F.V. Kyrychenko, J. Kono, X. Wei, S.A. Crooker, G.D. Sanders, D.H. Reitze, C.J. Stanton, and G.S. Solomon, Phys. Rev. B 72, 045340 (2005).
- [12] G.D. Sanders, Y. Sun, F.V. Kyrychenko, C.J. Stanton, G.A. Khodaparast, M.A. Zudov, J. Kono, Y.H. Matsuda, N. Miura, and H. Munkata, Phys. Rev. B 68, 165205 (2003).
- [13] W. Gempel, X. Pan, T. Kasturirachchi, G.D. Sanders, M. Edirisooriya, T.D. Mishima, R.E. Doezema, C.J. Stanton, and M.B. Santos, Springer Proceedings in Physics 119, 213 (2008).
- [14] In actuality, we solve the problem for a superlattice in the limiting case where the barrier is thick enough to prevent tunneling between the wells.